Loss of SMAD4 Promotes Colorectal Cancer Progression by Accumulation of Myeloid-Derived Suppressor Cells through CCL15-CCR1 Chemokine Axis

Susumu Inamoto[1,5], Yoshiro Itatani[1,2,5], Takamasa Yamamoto[1], Sachiko Minamiguchi[3],
Hideyo Hirai[4], Masayoshi Iwamoto[1], Suguru Hasegawa[1], Makoto Mark Taketo[1,2]
Yoshiharu Sakai[1], and Kenji Kawada[1]

Authors' Affiliations: [1]Departments of Surgery, [2]Pharmacology, [3]Diagnostic Pathology,
and [4]Transfusion Medicine & Cell Therapy, Graduate School of Medicine, Kyoto
University, Kyoto, Japan.
[5] S. Inamoto and Y. Itatani contributed equally to this article.

Corresponding authors: Kenji Kawada, Department of Surgery, Graduate School of
Medicine, Kyoto University, 54 Shogoin- Kawara-cho, Sakyo-ku, Kyoto, Japan, 606-8507.
Phone: +81-75-366-7595; FAX: +81-75-366-7642; E-mail: kkawada@kuhp.kyoto-u.ac.jp

Running title: MDSCs accumulate around SMAD4-negative CRC through
CCL15-CCR1 axis

Keywords: colorectal cancer, SMAD4, chemokine, CCR1, MDSC

Potential Conflict of Interest: No potential conflicts of interest were disclosed.

Word Counts: 4995 words

Figures and tables: 4 figures and 2 tables

Supplementary figures and tables: 4 supplementary figures and 3 supplementary

tables

Statement of translational relevance

Recent studies have revealed that bone marrow-derived myeloid cells play critical roles in cancer invasion and metastasis. However, most these findings were obtained from mouse models, and it has remained to be investigated whether similar mechanisms are actually involved in humans. This is the first clinical study showing that loss of the tumor suppressor SMAD4 promotes primary CRC progression by accumulation of CCR1^{+} myeloid cells to the invasion front through CCL15-CCR1 axis. This study has demonstrated that most of CCR1^{+} cells were of the granulocytic-myeloid derived suppressor cells (G-MDSCs) phenotype, and that serum CCL15 levels in CRC patients were significantly higher than in controls. These results may give a convincing justification for CCR1 inhibitors to prevent CRC metastasis as an adjuvant therapy after surgical resection of the primary CRC.

Abstract

Purpose: We previously reported loss of SMAD4 promotes chemokine CCL15 expression to recruit CCR1^{+} myeloid cells via the CCL15-CCR1 axis, which facilitates metastasis of colorectal cancer (CRC) to the liver. The purposes of this study are to investigate whether essentially the same mechanism works in tumor invasion of the primary CRC and to evaluate the clinical importance of CCL15 expression and CCR1^{+} cell accumulation.

Experimental Design: Using human CRC cell lines with reduced expression of SMAD4 or CCL15, we investigated tumor growth activities *in vivo*. We used immunohistochemistry (IHC) to investigate expression of SMAD4, CCL15 and CCR1 with 333 clinical specimens of primary CRC. We next characterized the CCR1^{+} cells using double immunofluorescence staining with several specific cell-type markers. Finally, we determined the serum CCL15 levels in 132 CRC patients.

Results: In an orthotopic xenograft model, CCL15 secreted from SMAD4-deficient CRC cells recruited CCR1^{+} cells, resulting in aggressive tumor growth. IHC indicated loss of SMAD4 was significantly associated with CCL15 expression, and that CCL15-positive primary CRCs recruited ~2.2 times more numbers of CCR1^{+} cells at their invasion front than CCL15-negative CRCs. Importantly, these CCR1^{+} cells were of the myeloid derived suppressor cell (MDSC) phenotype (CD11b^{+}, CD33^{+}, and HLA-DR^{-}). Most CCR1^{+} cells showed the granulocytic-MDSC phenotype (CD15^{+}), although some did the monocytic-MDSC phenotype (CD14^{+}). Serum CCL15 levels in CRC patients were significantly higher than in controls.

Conclusion: Blocking the recruitment of CCR1^{+} MDSCs may represent a novel molecular targeted therapy, and serum CCL15 concentration can be a novel biomarker for CRC.

Introduction

Colorectal cancer (CRC) develops progressively through accumulation of genetic alterations in genes including *APC*, *KRAS*, p53 (*TP53*), *SMAD4*, and transforming growth factor-β (TGF-β) receptor type II (*TGFBR2*), etc (1). SMAD4 is a pivotal transcription factor involved in TGF-β superfamily signaling (e.g., TGF-β, bone morphogenetic proteins (BMPs) and activins) and is an established tumor suppressor in CRC. Loss of SMAD4 is found in 20-40% of CRC, and is strongly correlated with the prognosis of CRC patients (2-4). As a model for invasive colon cancer, we previously constructed *cis-Apc+/Δ716 Smad4+/−* (*Apc/Smad4*) mice by inducing loss of *Apc* and *Smad4* in the epithelium (5, 6). In the *Apc/Smad4* tumors, a C-C chemokine CCL9 is secreted from tumor cells and attracts CCR1^{+} myeloid cells from the bone marrow to the invasion front where CCR1^{+} myeloid cells promote tumor invasion by secreting matrix metalloproteinase 9 (MMP9) and MMP2 (6). Using a mouse model of CRC liver metastasis, we also demonstrated that CCL9-expressing CRC cell lines recruit CCR1^{+} myeloid cells to expand metastatic foci in the liver (7), and that four distinct types of myeloid cells are recruited to the metastatic foci; CCR1^{+} neutrophils, eosinophils monocytes and fibrocytes (8). In addition to these mouse models, we recently reported that SMAD4 binds directly to the promoter region of human *CCL15* (a human ortholog of mouse *CCL9*) and negatively regulates its expression *in vitro* (9). In addition, with human specimens of liver metastasis of CRC, we also showed that loss of SMAD4 in CRC cells promotes CCL15 expression, recruits CCR1^{+} myeloid cells, and facilitates liver metastasis (9). However, it has not been investigated whether CCL15-CCR1 chemokine axis is correlated with progression of primary CRC. Likewise, these CCR1^{+} myeloid cells remain to be characterized further.

Tumor cells often acquire the capability of survival and invasion by activating oncogenic pathways or inactivating tumor suppressor pathways. In addition to these cell-autonomous changes in the epithelial compartment, the stromal compartment plays key roles in cancer progression. In particular, bone marrow-derived (i.e., myeloid) cells

5

constitute the major components of the tumor microenvironment, and attract rising attention as key players for malignant progression (10, 11). Namely, tumor-associated macrophages, neutrophils, and myeloid-derived suppressor cells (MDSCs) can enhance tumor progression by facilitating the growth and migration of tumor cells, angiogenesis, and/or suppression of immune response. MDSCs constitute a heterogeneous population of immature myeloid cells that are increased in cancer, inflammation and infection. In mice, MDSCs express myeloid markers (Gr1$^+$ and CD11b$^+$). In humans, the Gr1 antigen is absent, and human MDSCs are defined as cells expressing myeloid cell markers such as CD11b and CD33 but lacking HLA-DR (12, 13). Human MDSCs comprise two subtype populations; monocytic MDSCs and granulocytic MDSCs. Human monocytic-MDSCs are usually characterized as HLA-DR$^-$, CD11b$^+$, CD33$^+$ and CD14$^+$, whereas granulocytic-MDSCs are as HLA-DR$^-$, CD11b$^+$, CD33$^+$ and CD15$^+$ (12, 13). Because the phenotype and action mechanisms of MDSCs appear to be tumor type-dependent, it is important to characterize all MDSC subsets with clinical relevance.

Here we report that in human primary CRC, loss of SMAD4 is correlated with CCL15 expression and concomitant accumulation of CCR1$^+$ cells at the invasion front. These CCR1$^+$ cells are of the MDSC phenotype, and most of them show the granulocytic-MDSC phenotype, although some have the monocytic-MDSC phenotype. They express MMP2, MMP9, inducible nitric oxide synthase (iNOS), Arginase-1 (ARG1) and indoleamine 2,3- dioxygenase (IDO). Importantly, Stage II/III patients with CCL15-positive primary CRC tend to have a shorter relapse-free survival (RFS) than those with CCL15-negative CRC (P = 0.15), although not a significant difference. We also find that the serum CCL15 concentration of preoperative CRC patients is higher than that of controls, and that the level increases significantly already in relatively early stages. In a mouse orthotopic xenograft model, we demonstrate that CCL15 secreted from SMAD4-deficient CRC cells recruits CCR1$^+$ cells and promotes tumor growth, whereas overexpression of SMAD4 or knockdown of CCL15 diminishes CCR1$^+$ cell accumulation and suppresses tumor growth. Taken together, these results suggest that

6

blocking the CCL15-CCR1 axis may be an efficacious therapeutic strategy for CRC

patients, and that the serum CCL15 concentration may be a novel molecular biomarker

for CRC.

Materials and Methods

Patients population

  A total of 333 CRC patients underwent primary resection at Kyoto University Hospital between June 2005 and December 2008, and their tissue samples were retrospectively analyzed. For the analysis of serum CCL15 level, preoperative serum samples were collected from 132 CRC patients and 20 healthy controls between November 2011 and February 2014. The diagnosis of CRC was confirmed by pathological examination. These study protocols were approved by the institutional review board of Kyoto University, and patients provided their consents for data analysis.

Cell lines and reagents

  HT29 and Colo205 cells were supplied from American Type Culture Collection (ATCC) in the year 2011 during study initiation and were maintained in low glucose DMEM or RPMI with 10% FBS and 1% penicillin/streptomycin mixture. All cell lines were authenticated by TAKARA Bio Inc (Shiga, Japan) using DNA profiling of short tandem repeat markers and further verified by morphology and/or flow cytometry on July, 2014. They were routinely tested negative for *mycoplasma*.

Immunohistochemistry (IHC) analysis

  Formalin-fixed, paraffin-embedded sections were stained with respective antibodies (Supplementary Table S1) by the avidin-biotin immunoperoxidase method. The expression of SMAD4 was evaluated as a nuclear staining, and the percentage of positively stained cells was scored as follows: –, < 5%; +, 5-9%; ++, 10-34%; +++, ≥ 35%, as previously described (2). The presence of CCL15 protein was interpreted as positive when > 10% of the tumor cells at the invasion front were stained. We quantified the densities of CCR1$^+$ cells and CCR3$^+$ cells at the invasion front of primary CRC (5-9 fields (0.1mm^2) analyzed per one sample), as previously described (9). We adopted IHC analysis of MLH1 and MSH2, and then interpreted as mismatch repair intact (MMR-I)

8

when both proteins were positive, while as MMR deficient (MMR-D) when either protein was negative (14). One experienced pathologist (SM) and two researchers (SI and TY) independently evaluated all IHC samples without prior knowledge of other data. The slides with different evaluations among them were interpreted once again followed by a conclusive judgment.

Immunofluorescence analysis

For Immunofluorescence analyses of α-SMA, CCR1, CCR2, CXCR2, CD3, CD8, CD14, CD15, CD31, CD33, CD68, MPO, HLA-DR, iNOS, ARG1, IDO, MMP2, and MMP9, we prepared archival formalin-fixed, paraffin-embedded CCR1$^+$ cells-accumulated primary CRC tissue samples, which sliced in 4μm. After deparaffinization, heat induced antigen retrieval was performed. 1st antibodies (Supplementary Table S1) was applied and incubated overnight at 4℃. After fluorescent labeling 2nd antibodies were applied (Alexa Fluor 488 anti-mouse or anti-goat and 594 anti-rabbit), slides were mounted with Mounting Medium including DAPI. Representative figures were taken by fluorescence microscope.

Statistical analysis

All values are expressed as means ± standard deviation (SD). Categorical data were determined using Fisher's exact test. Continuous variables were determined using Student's *t*-test or Mann-Whitney *U* test. Dunnett's test was also used for multiple comparisons. To determine factors associated with CCL15 expression, multivariate logistic regression analysis was used and factors with a *P* value of < 0.10 were included in the model. Survival curves were calculated according to the method of Kaplan and Meier, and analyzed using the log-rank test. All analyses were two-sided, and a *P* value of < 0.05 was considered statistically significant. Statistical analyses were performed using the JMP Pro software, version11.0.0 (SAS Institute Inc, NC, USA).

9

Results

Loss of SMAD4 causes recruitment of CCR1^{+} cells through CCL15-CCR1 signaling to promote tumor growth in a mouse model

Loss of SMAD4 expression is associated with malignant progression of CRC (2-5). We previously reported that colon tumors of *Apc/Smad4*-deficient mice, a mouse model of invasive CRC, express chemokine CCL9 to recruit CCR1^{+} myeloid cells, which promotes tumor invasion (6). Therefore, we hypothesized that expression of its human ortholog CCL15 also promotes tumor invasion through CCL15-CCR1 signaling in human primary CRC.

To test the hypothesis, we first examined the role of CCL15 *in vivo* using an orthotopic xenograft model. We inoculated luciferase (Luc)-expressing human CRC cells into the rectal submucosa of nude mice and monitored the tumor growth by bioluminescence, which enabled quantification of the tumor cells by photon counting. A SMAD4-deficient CRC cell line, HT29, constitutively expressed high levels of CCL15 (9). When cMyc-tagged SMAD4 was stably over-expressed in HT29 cells (Luc-HT29 cMyc-*SMAD4*) by lentiviral transduction, CCL15 secretion was significantly decreased to ~1/5 of that from the control cells (Fig. 1A) without affecting cell viability (9). We also confirmed that CCL15 secretion was significantly decreased by over-expressing SMAD4 in another SMAD4-deficient CRC cell line Colo205 cells, although to a less extent than in HT29 cells (Supplementary Fig. S1A). When Luc-HT29 cMyc-*SMAD4* cells were inoculated into nude mice, their luciferase activity significantly decreased compared with those of control cells (Fig. 1B). Upon histological examination, we verified that Luc-HT29 cMyc-tag control cells expressed CCL15 and accumulated CCR1^{+} cells around the primary tumors, whereas Luc-HT29 cMyc-*SMAD4* cells did not (Fig. 1C). To investigate the role of CCL15 *in vivo*, we established HT29 cells engineered with stable CCL15 knockdown (Luc-HT29 sh*CCL15*). Two independent sh*CCL15* constructs (sh*CCL15* #1 and #2) decreased CCL15 expression significantly (Fig. 1D) without affecting cell viability (Supplementary Fig. S1B). When Luc-HT29 sh*CCL15* cells were inoculated into nude

10

mice, their luciferase activity markedly decreased compared with that of control cells (Fig. 1E). As anticipated, we verified by IHC analysis that Luc-HT29 sh*CCL15* cells lacked CCL15 expression and accumulated few CCR1^{+} cells around the primary tumors (Fig. 1F). Taken together, loss of SMAD4 and expression of CCL15 promote CRC progression in an orthotopic xenograft model.

CCL15 expression is associated with loss of SMAD4 and the accumulation of CCR1^{+} cells, which results in tumor invasion and poorer prognosis

To confirm the clinical relevance of the above results, we investigated expression of SMAD4, CCL15 and CCR1 with 333 clinical specimens of primary CRC obtained between 2005 and 2008 (Stage 0, *n* = 10; Stage I, *n* = 59; Stage II, *n* = 117; Stage III, *n* = 91; Stage IV, *n* = 56) (Supplementary Fig. 2A left). IHC analysis indicated that CCL15 was expressed in tumor cells mainly at the invasion front, not at the center of the whole tumor (Fig. 2A), and that CCL15 expression was positive in 71% (238 of 333), which is quite similar to the frequency in liver metastases of CRC (9). Univariate analysis of each clinicopathological factor indicated that CCL15 expression was correlated with histology (*P* = 0.05), vascular invasion (*P* = 0.05) and SMAD4 expression (*P* < 0.01) (Table 1). In the multivariate analysis including factors with a *P* value of < 0.10, only SMAD4 expression remained significantly correlated with CCL15 expression (Table 2; odds ratio, 1.94; 95% confidence interval, 1.16-3.31; *P* = 0.01), which indicated a significant inverse correlation between CCL15 and SMAD4. Regarding the Stage-based and T factor-based classifications, CCL15 was highly expressed in Stage II/III (73.5% and 79.1 %, respectively) and T2/T3 (76.9 % and 75.7 %, respectively) (Supplementary Table S2), although CCL15 tended to decrease in Stage IV and T4. To evaluate the clinical outcome of CCL15 expression in primary CRC, we analyzed RFS of 299 patients who underwent curative resection (Supplementary Fig. 2A right). Statistical analyses showed that Stage II/III patients with CCL15-positive CRC tended to exhibit a shorter RFS than those with CCL15-negative CRC (*P* = 0.15), although not a significant difference. Similar tendency

11

was not found in the analysis for patients of Stages 0-IV combined (Fig. 2B). It was recently reported that microsatellite instability (MSI)-high and SMAD4 expression were identified as independent prognostic factors for better prognosis in Stage II/III colon cancer patients from a large randomized phase III trial (3). Therefore, we also analyzed the effect of MSI/MMR status and SMAD4 expression in Stage II/III patients of this study, and found that neither MSI/MMR status nor SMAD4 expression was significantly correlated with RFS (Supplementary Fig. S2B and S2C).

Next, we investigated the relationship between CCL15 expression and CCR1^{+} cell accumulation, and found that significant numbers of CCR1^{+} cells accumulated at the invasion front of CCL15-positive CRC, but few around CCL15-negative CRC (Fig. 2A). Quantification of the density of CCR1^{+} cells indicated that the number of CCR1^{+} cells around CCL15-positive CRC was ~2.2 times higher than that around CCL15-negative ones (22.4 $\pm$ 24.7 vs.49.7 $\pm$ 30.9; $P < 0.01$; Fig. 2C), which is in agreement with the data observed in liver metastases of CRC (9). We also found that the accumulation of CCR1^{+} cells was especially high in Stage I/II and T2/T3, but it diminished in Stage III/IV and T4 (Fig. 2D), which was similar to the expression pattern of CCL15 (Supplementary Table S2). Taken together, these results suggest that CCL15 expression is associated with loss of SMAD4 and the accumulation of CCR1^{+} cells, which may result in tumor invasion of T2/T3 CRC and poorer prognosis of Stage II/III CRC.

Characterization of CCR1^{+} cells accumulated around primary CRC

We previously reported that CCR1^{+} cells accumulating around liver metastases of CRC expressed the myeloid cell markers CD11b and myeloperoxidase (MPO), and also produced MMP9 (9). Therefore, we next characterized the CCR1^{+} cells accumulating around the primary CRC using double immunofluorescence staining with several specific cell-type markers. We found that these CCR1^{+} cells were positive for CD11b, CD33, MPO and CD68, while they were negative for HLA-DR, CD3, CD8, CD31 and α-SMA (Fig. 3A-D and Supplementary Fig. S3A-E), which suggests that they are so-called

12

"myeloid-derived suppressor cells" (MDSCs; CD33^{+}, CD11b^{+}, HLA-DR^{-} populations) (12, 13). MDSCs constitute a heterogeneous population of myeloid cells, and comprise two subtype populations; CD15^{+} granulocytic-MDSCs and CD14^{+} monocytic-MDSCs (12, 13). Importantly, majority of these CCR1^{+} cells were also positive for CD15 (Fig. 3E), and only a minor fraction (~ 10%) were positive for CD14 (Fig. 3F), which suggests that these CCR1^{+} cells constitute two subpopulations; granulocytic-MDSCs and monocytic-MDSCs.

In the tumor microenvironment, MDSCs are characterized by immunosuppressive function (by producing ARG1, iNOS, and IDO) and angiogenic function (by producing MMP) (12, 13). We further confirmed that these CCR1^{+} cells expressed ARG, iNOS, and IDO in addition to MMP2 and MMP9 (Fig. 3G, H and Supplementary Fig. S3F-H). Moreover, a subpopulation of these CCR1^{+} cells was positive for CCR2 and CXCR2 (Supplementary Fig. S3I and J) that are major chemokine receptors expressed on MDSCs (15, 23). These results suggest that CCR1^{+} cells accumulating around the primary CRC are composed of mainly granulocytic-MDSCs and partially monocytic-MDSCs.

Serum CCL15 concentration is a novel biomarker of CRC

It was recently reported that serum CCL15 was identified as a specific biomarker for hepatocellular carcinoma (16) and lung cancer (17). Therefore, we investigated whether the serum CCL15 level could also be a biomarker for CRC progression. We prospectively collected preoperative serum samples from another cohort of 132 CRC patients and 20 healthy controls between 2011 and 2014 (Supplementary Table S3), and then measured the CCL15 concentration by ELISA. The serum CCL15 concentration was significantly higher in CRC patients than in controls (17.8 ± 7.9 vs 9.4 ± 3.0 ng/ml, respectively; $P < 0.01$; Fig. 4A). Regarding the threshold for differentiation, the sensitivity and specificity were 78.8 % (104 of 132) and 70.0 % (14 of 20), respectively, with a cutoff value of 10.5 ng/ml. We then investigated the Stage-based and TNM-based

13

classifications of the serum CCL15 concentration, and found that the concentration was significantly increased from a relatively early stage (Fig. 4B and C), which was similar to the expression pattern in the primary CRC (Fig. 2D). Taken together, serum CCL15 may be a prognostic biomarker as well as a therapeutic biomarker for inhibition of CCR1-CCL15 signaling.

14

Discussion

TGF-β signaling has both tumor-suppressive and pro-oncogenic effects depending on the tumor type. The nature of the switch that determines the TGF-β functions between a tumor suppressor and a tumor promoter has attracted intense research (18). SMAD4-independent TGF-β pathway coupled with loss of SMAD4 was reported to be involved in the tumor-promoting effects of TGF-β such as epithelial-to-mesenchymal transition, migration, invasion, tumorigenicity and metastasis (19, 20). In addition, it was recently reported that loss of SMAD4 activates SMAD4-independent BMP signaling to promote CRC metastasis via activation of Rho and ROCK (21). In addition to the cell-autonomous changes in cancer cells, the crosstalk between cancer cells and stromal cells plays key roles in malignant progression. For example, IL-11 secreted by TGF-β-stimulated cancer-associated fibroblasts triggers GP130/STAT3 in CRC cells to promote metastasis (22). We previously reported that loss of SMAD4 promotes CCL15 expression to recruit CCR1^{+} myeloid cells and facilitate liver metastasis of CRC (9).

To our knowledge, this is the first demonstration that a genetic event (i.e., loss of *SMAD4* gene) can promote chemokine production that results in tumor metastasis. In this study, we have shown that essentially the same mechanism takes place in the primary CRC. Several previous studies showed that loss of SMAD4 is significantly correlated with poorer prognosis in CRC patients (3, 4), but we did not find any correlation in this retrospective study (Supplementary Fig. S2B). One of the reasons for this discrepancy may be that our cohort study showed relatively better prognosis than previous reports (Supplementary Fig. S2A; 5-year overall survival and RFS were ~80% and ~70%, respectively, even in Stage III), resulting the smaller difference between the SMAD4-positive and SMAD4-negative ones. Therefore, it may be notable that Stage II/III patients with CCL15-positive CRC tended to exhibit a shorter RFS than those with CCL15-negative CRC (Fig. 2B).

Tumor microenvironment contains several types of cells including cancer epithelial

15

cells and normal host cells. The MDSC population is one of the important stromal constituents that play key roles in malignant progression (12, 13). Here we have shown that CCL15 expression caused by loss of SMAD4 in tumor cells helps recruitment of CCR1$^+$ cells at the invasion front of primary CRC (Fig. 4D). These CCR1$^+$ cells were positive for CD33, CD11b and MPO (Fig. 3A, B and D), and negative for CD3, CD8, HLA-DR, α-SMA and CD31 (Fig. 3C, Supplementary Fig. S3A, B, C and D), suggesting that they are of the myeloid origin, but not derived from lymphocytes, fibroblasts or endothelial cells. Moreover, they expressed both immature myeloid cell marker (positive for CD33) and mature myeloid cell markers (positive for MPO and CD68) (Supplementary Fig. S3E). Importantly, they expressed not only granulocyte-lineage markers (MPO and CD15) (Fig. 3E), known for granulocytic-MDSCs, but also monocyte-lineage markers (CD68 and CD14) (Fig. 3F), for monocytic-MDSCs, indicating that these CCR1$^+$ cells constitute a heterogeneous population composed of granulocytic-MDSCs and monocytic-MDSCs, although further analysis is needed to identify the functions of each subpopulation. These cells may contribute the development of tumor microenvironment through production of MMP2, MMP9, iNOS, ARG1, and IDO (Fig. 3G and H, Supplementary Fig. S3F, G, and H). We observed that more numbers of CCR1$^+$ cells were accumulated at T2/T3 stage, suggesting that CRC cells use CCL15-CCR1 signaling to invade through tightly connected tissue, muscularis propria (MP) layer. It has been reported that MDSCs express some chemokine receptors such as CCR2 and CXCR2 in several types of cancers (15, 23). We observed that a certain proportion of these CCR1$^+$ cells were also positive for CCR2 and CXCR2 (Supplementary Fig. S3I and J), which may suggest that the phenotype and function of MDSC subsets are tumor type- and organ-dependent.

Chemokine CCL15 shows a strong chemotactic activity for myeloid-lineage cells, including monocytes, neutrophils, and dendritic cells but also for some T lymphocytes to bind CCR1 and/or CCR3 (24). CCL15 is highly expressed in certain leukocytes and macrophages (24), and is converted into potent chemoattractants by MMPs and other

16

serine proteases released during inflammatory responses (25). We also examined the expression of CCR3 with the same 333 clinical specimens of primary CRC, and found that CCR3$^+$ cell accumulation was rarely observed around the primary CRCs (Supplementary Fig. S4A). Quantification of the density of CCR3$^+$ cells indicated that the number of CCR3$^+$ cells around CCL15-positive CRCs was 11.4 $\pm$ 7.2, while that around CCL15-negative ones was 12.1 $\pm$ 8.3 (P = 0.80), suggesting there was no significant correlation between CCL15 and CCR3 (Supplementary Fig. S4B). CCR3$^+$ cell accumulation was not correlated with SMAD4 expression (P = 0.63; Supplementary Fig. S4C), and CCR1$^+$ cell accumulation (P = 0.57; Pearson's correlation coefficients; Supplementary Fig. S4D). Although CCL15 is an agonist of CCR1 and CCR3, CCL15 is reported to have a higher affinity for the CCR1 compared with CCR3 (24, 26, 27). Taken together with our results, we propose that CCR1 can be the major receptor for CCL15 in vivo. Regarding the molecular mechanism of CCL15 expression, we previously showed that SMAD4 binds directly to the promoter region of human *CCL15* gene to negatively regulate its expression through TGF-β family signaling (9). We also observed that CCL15 expression is inversely correlated with SMAD4 expression in clinical specimens of human CRC liver metastases (9). In this study, we have verified in the primary CRC that there is a significant inverse correlation between CCL15 and SMAD4 levels by IHC analysis of 333 clinical (Table 1 and 2). Loss of SMAD4 was found in 41% (136 of 333), whereas CCL15 expression was positive in 71% (238 of 333). Because the difference between these frequencies was about 30%, we speculate that SMAD4 is the central regulator of CCL15 expression, although factors other than SMAD4 can also contribute to CCL15 expression. It is noteworthy that CCL15 was identified in the serum samples of hepatocellular carcinoma patients as a specific proteomic biomarker using SELDI-TOF-MS system (16). In addition, CCL15 was recently reported to be the most significant serum marker associated with short survival in early-stage (i.e., Stage I/II) lung cancer (17). In our cohort study, we have also observed that Stage II/III patients with CCL15-positive CRC tend to exhibit a shorter RFS than those with CCL15-negative CRC

17

(P = 0.15) (Fig. 2B), which suggests that CCL15 expression within tumors may be associated with the clinical prognosis of several types of cancer. We previously reported in mouse models that tumor invasion and metastasis are suppressed by inhibiting CCL15-CCR1 signaling with a CCR1 inhibitor, genetic knockdown of *CCL15* gene, or introduction of *CCR1* knockout mutation (6, 7, 9). Some CCR1 inhibitors have already been used in phase I/II clinical trials for the patients with rheumatoid arthritis, chronic obstructive pulmonary disease and multiple sclerosis (28), although they have not yet been employed for anti-cancer treatment. Selectively targeting CCR1^{+} MDSCs, perhaps in combination with conventional chemotherapy regimens, can be a novel molecular targeted strategy, and the serum CCL15 concentration may serve as a novel biomarker for CRC patients. In particular, patients with a high CCL15 concentration could benefit from CCR1 inhibition therapy.

Authors' Contributors

Conception and design: K. Kawada, M. Mark. Taketo, Y. Sakai

Development of methodology: K, Kawada

Acquisition of data: S. Inamoto, Y. Itatani, S. Minamiguchi

Analysis and interpretation of data: S. Inamoto, Y. Itatani, K. Kawada

Writing, review, and/or revision of the manuscript: S. Inamoto, Y. Itatani, H. Hirai, M. Mark. Taketo, K. Kawada

Administrative, technical, or material support: T. Yamamoto, M. Iwamoto, S. Hasegawa, S. Minamiguchi

Study supervision: M. Mark. Taketo, Y. Sakai

References

1. Weinberg RA. Multi-step tumorigenesis. The biology of cancer (Garland Science) 2007;11:399-462.

2. Salovaara R, Roth S, Loukola A, Launonen V, Sistonen P, Avizienyte E, et al. Frequent loss of SMAD4/DPC4 protein in colorectal cancers. Gut 2002;51:56–59.

3. Roth AD, Delorenzi M, Tejpar S, Yan P, Klingbiel D, Fiocca R, et al. Integrated analysis of molecular and clinical prognostic factors in stage II/III colon cancer. J Natl Cancer Inst 2012;104:1635-46.

4. Alazzouzi H, Alhopuro P, Salovaara R, Sammalkorpi H, Järvinen H, Mecklin JP, et al. SMAD4 as a prognostic marker in colorectal cancer. Clin Cancer Res 2005;11:2606-2611.

5. Takaku K, Oshima M, Miyoshi H, Matsui M, Seldin MF, Taketo MM. Intestinal tumorigenesis in compound mutant mice of both Dpc4 (Smad4) and Apc genes. Cell 1998;92:645–656.

6. Kitamura T, Kometani K, Hashida H, Matsunaga A, Miyoshi H, Hosogi H, et al. SMAD4-deficient intestinal tumors recruit CCR1+ myeloid cells that promote invasion. Nat Genet 2007;39:467–475.

7. Kitamura T, Fujishita T, Loetscher P, Revesz L, Hashida H, Kizaka-Kondoh S, et al. Inactivation of chemokine (C-C motif) receptor 1 (CCR1) suppresses colon cancer liver metastasis by blocking accumulation of immature myeloid cells in a mouse model. Proc Natl Acad Sci USA 2010;107:13063–13068.

8. Hirai H, Fujishita T, Kurimoto K, Miyachi H, Kitano S, Inamoto S, et al. CCR1-mediated accumulation of myeloid cells in the liver microenvironment promoting mouse colon cancer metastasis. Clin Exp Metastasis 2014;31:977-989.

9. Itatani Y, Kawada K, Fujishita T, Kakizaki F, Hirai H, Matsumoto T, et al. Loss of SMAD4 from colorectal cancer cells promotes CCL15 expression to recruit CCR1+ myeloid cells and facilitate liver metastasis. Gastroenterology 2013;145:1064-1075.

10. Murdoch C, Muthana M, Coffelt SB, Lewis CE. The role of myeloid cells in the

20

promotion of tumor angiogenesis. Nat Rev Cancer 2008;8:618-631.

11. Joyce JA, Pollard JW. Microenvironmental regulation of metastasis. Nat Rev Cancer 2009;9:239-252.

12. Talmadge JE, Gabrilovich DI. History of myeloid-derived suppressor cells. Nat Rev Cancer 2013;13:739-52.

13. Gabrilovich DI, Ostrand-Rosenberg S, Bronte V. Coordinated regulation of myeloid cells by tumours. Nat Rev Immunol 2012;12:253-68.

14. Bertagnolli MM, Niedzwiecki D, Compton CC, Hahn HP, Hall M, Damas B, et al. Microsatellite instability predicts improved response to adjuvant therapy with irinotecan, fluorouracil, and leucovorin in stage III colon cancer: Cancer and Leukemia Group B Protocol 89803. J Clin Oncol 2009;27:1814-21.

15. Lesokhin AM, Hohl TM, Kitano S, Cortez C, Hirschhorn-Cymerman D, Avogadri F, et al. Monocytic CCR2(+) myeloid-derived suppressor cells promote immune escape by limiting activated CD8 T-cell infiltration into the tumor microenvironment. Cancer Res 2012;72:876-886.

16. Li Y, Wu J, Zhang W, Zhang N, Guo H. Identification of serum CCL15 in hepatocellular carcinoma. Br J Cancer 2013;108:99-106.

17. Bodelon C, Polley MY, Kemp TJ, Pesatori AC, McShane LM, Caporaso NE, et al. Circulating levels of immune and inflammatory markers and long versus short survival in early-stage lung cancer. Ann Oncol 2013;24:2073-9.

18. Massagué J. TGFbeta in Cancer. Cell 2008;134:215-30.

19. Zhang B, Halder SK, Kashikar ND, Cho YJ, Datta A, Gorden DL, et al. Antimetastatic role of Smad4 signaling in colorectal cancer. Gastroenterology 2010;138:969-80.

20. Pino MS, Kikuchi H, Zeng M, Herraiz MT, Sperduti I, Berger D, et al. Epithelial to mesenchymal transition is impaired in colon cancer cells with microsatellite instability. Gastroenterology 2010;138:1406-17.

21. Voorneveld PW, Kodach LL, Jacobs RJ, Liv N, Zonnevylle AC, Hoogenboom JP, et

21

al. Loss of SMAD4 alters BMP signaling to promote colorectal cancer cell metastasis via activation of Rho and ROCK. Gastroenterology 2014;147:196-208.

22. Calon A, Espinet E, Palomo-Ponce S, Tauriello DVF, Iglesias M, Céspedes MV, et al. Dependency of colorectal cancer on a TGF-β-driven program in stromal cells for metastasis initiation. Cancer Cell 2012;22:571-84.

23. Katoh H, Wang D, Daikoku T, Sun H, Dey SK, DuBois RN. CXCR2-expressing myeloid-derived suppressor cells are essential to promote colitis-associated tumorigenesis. Cancer Cell 2013;24:631-44.

24. Forssmann U, Magert HJ, Adermann K, Escher SE, Forssmann WG. Hemofiltrate CC chemokines with unique biochemical proterties: HCC-1/CCL14a and HCC2/CCL15. J Leukoc Biol 2001;70;357-366.

25. Starr AE, Dufour A, Maier J, Overall CM. Biochemical analysis of matrix metalloproteinase activation of chemokines CCL15 and CCL23 and increased glycosaminoglycan binding of CCL16. J Biol Chem 2012;287:5848-60.

26. Youn BS, Zhang SM, Lee EK, Park DH, Broxmeyer HE, Murphy PM, et al. Molecular cloning of leukotactin-1: a novel human beta-chemokine, a chemoattractant for neutrophils, monocytes, and lymphocytes, and a potent agonist at CC chemokine receptors 1 and 3. J Immunol 1997;159;5201-5.

27. Escher SE, Forssmann U, Frimpong-Boateng A, Adermann K, Vakili J, Sticht H, et al. Functional analysis of chemically synthesized derivatives of the human CC chemokine CCL15/HCC-2, a high affinity CCR1 ligand. J Pept Res 2004;63;36-47.

28. Gladue RP, Brown MF, Zwillich SH. CCR1 antagonists: what have we learned from clinical trials. Curr Top Med Chem 2010;10:1268-77.

Table 1. Univariate analysis of clinicopathological factors (n = 333)

Variables	CCL15 expression		P-value
	- (n = 95)	+ (n = 238)	
Age, years			0.48
Mean ± SD	66.9 ± 11.5	68.1± 10.4	
Sex			0.32
Male	55	153	
Female	40	85	
Location			0.49
Colon	67	177	
Rectum	28	61	
Histology			0.05
tub1 / tub2	84	226	
others	11	12	
T factor			0.33
Tis / T1 / T2	28	57	
T3 / T4	67	181	
N factor			0.39
Negative	61	140	
Positive	34	98	
M factor			0.20
Negative	75	202	
Positive	20	36	
UICC-TNM Stage			0.54
0, I, II	56	130	
III, IV	39	108	
Lymphatic invasion			0.71
Negative	55	143	
Positive	40	95	
Venous invasion			0.05
Negative	50	96	
Positive	45	142	
Microsatellite status			0.16
MMR-D	13	20	
MMR-I	82	218	
Neutrophil / lymphocyte ratio			0.28
< 5	84	220	
≥ 5	11	18	
CEA, ng/mL			0.22
< 5	51	146	
≥ 5	44	92	
CA19-9, U/mL			0.31
< 37	84	198	
≥ 37	11	40	
SMAD4 expression			< 0.01
Negative (-)	27	109	
Positive (+, ++, +++)	68	129	

23

Table 2. Multivariate analysis of factors associated with CCL15 expression

Variables	OR	95% CI	*P*-value
Histology (tub1 / tub2)	2.19	0.90 to 5.25	0.08
Venous invasion (Positive)	1.52	0.93 to 2.49	0.09
SMAD4 expression (Negative)	1.94	1.16 to 3.31	0.01

Abbreviations: OR, odds ratio; CI, confidence interval

24

Figure legends

Figure 1. Mouse orthotopic xenograft model for primary CRC.

A, ELISA showing CCL15 levels in the conditioned media when SMAD4 was overexpressed in Luc-HT29 cells. Mean; bars, ± SD. (Student's *t*-test; *, *P* < 0.01). B, In vivo bioluminescence images of mice inoculated with Luc-HT29 cells into rectal submucosa (left). Quantification of the orthotopic xenografts (photon counts) (right). Mean; bars, ± SD. (Student's *t*-test and Dunnett's test; *, *P* < 0.01). *n* = 4-10 for each group. C, IHC analysis of mouse rectums with orthotopic xenografts. Scale bar, 100 μm. D, ELISA showing CCL15 concentration of conditioned medium when *CCL15* was stably knockdown in Luc-HT29 cells. Mean; bars, ± SD. (Student's *t*-test; *, *P* < 0.01). E, In vivo bioluminescence images of mice inoculated with Luc-HT29 cells into rectal submucosa (left). Quantification of the orthotopic xenografts (photon counts) (right). Mean; bars, ± SD. (Student's *t*-test and Dunnett's test; *, *P* < 0.01). *n* = 4-10 for each group. F, IHC analysis of mouse rectums with orthotopic xenograft. Scale bar, 100 μm.

Figure 2. Correlation of SMAD4, CCL15, and CCR1^{+} cell accumulation in primary CRC.

A, Haematoxylin and eosin staining (H&E) and IHC staining for SMAD4, CCL15 and CCR1 of primary CRC specimens. Upper and lower panels show serial sections of representative SMAD4-deficient and SMAD4-expressing CRC, respectively. Scale bar, 100 μm. B, Effect of CCL15 expression on RFS in CRC patients who underwent curative resection of Stage 0-IV (left) and Stage II/III CRC (right) (Kaplan-Meier estimates). C, Quantification of the CCR1^{+} cell density in primary CRC with and without CCL15 expression (*n* = 238 and 95, respectively). *, *P* < 0.01; Mann-Whitney *U* test; horizontal bands show the means. D, Quantification of the CCR1^{+} cell density in primary CRC according to the Stage-based (left) and T factor-based (right) classifications. **, *P* < 0.05; Mann-Whitney *U* test and Dunnett's test; horizontal bands show the means.

25

Figure 3. Characterization of CCR1^{+} cells in the tumor microenvironment of primary CRC.

Clinical specimens from 8 CRC patients (Stage I, n = 2; Stage II, n = 5; Stage III, n = 1) were analyzed. Immunofluorescence staining for CCR1 and A, CD33, B, CD11b, C, HLA-DR, D, MPO, E, CD15, F, CD14, G, MMP9, and H, ARG1. Scale bar, 20 μm.

Figure 4. Serum CCL15 concentration of preoperative CRC patients.

A, ELISA for serum CCL15 concentration of preoperative CRC patients and healthy controls (n = 132 and 20, respectively). *, $P < 0.01$; Mann-Whitney U test; horizontal bands show the means. B, ELISA for serum CCL15 concentration of preoperative CRC patients according to the Stage-based classifications. *, $P < 0.01$; Mann-Whitney U test and Dunnett's test; horizontal bands show the means. C, ELISA for serum CCL15 concentration of preoperative CRC patients according to the T factor-, N factor- and M factor-based classifications. *, $P < 0.01$; Mann-Whitney U test and Dunnett's test; horizontal bands show the means. D, Schematic representation of the CCL15-CCR1 chemokine axis in primary CRCs. In SMAD4-positive primary CRCs, only a few MDSCs accumulate around their invasion front (left). In SMAD4-negative primary CRCs, CCL15 secreted from CRC cells recruits CCR1^{+} MDSCs, mainly G-MDSCs, around their invasion front. Accumulated CCR1^{+} MDSCs facilitate tumor invasion through immunosuppressive function (by producing ARG1, iNOS, and IDO) and tissue-destructive and angiogenic function (by producing MMP2 and MMP9) (right).
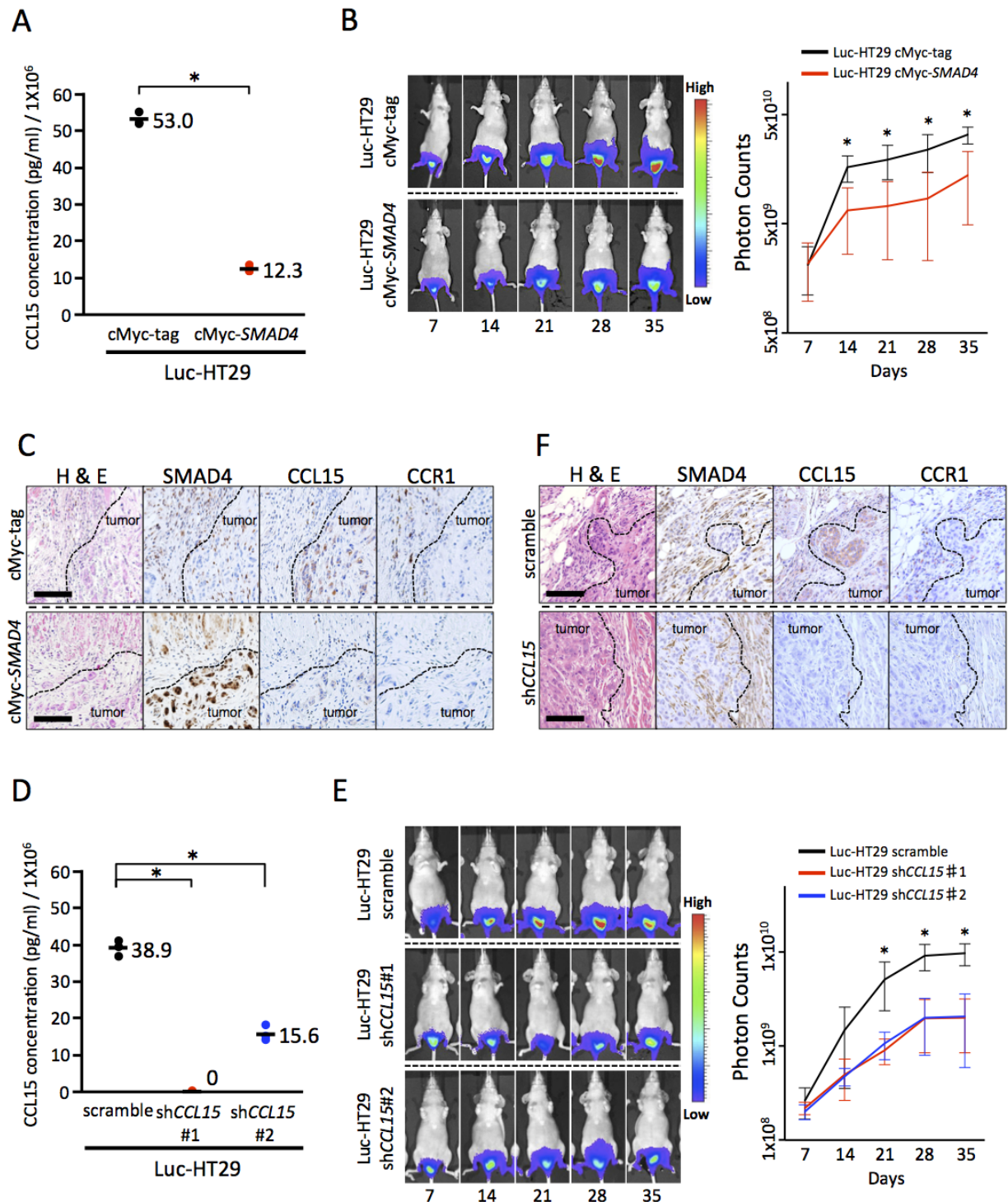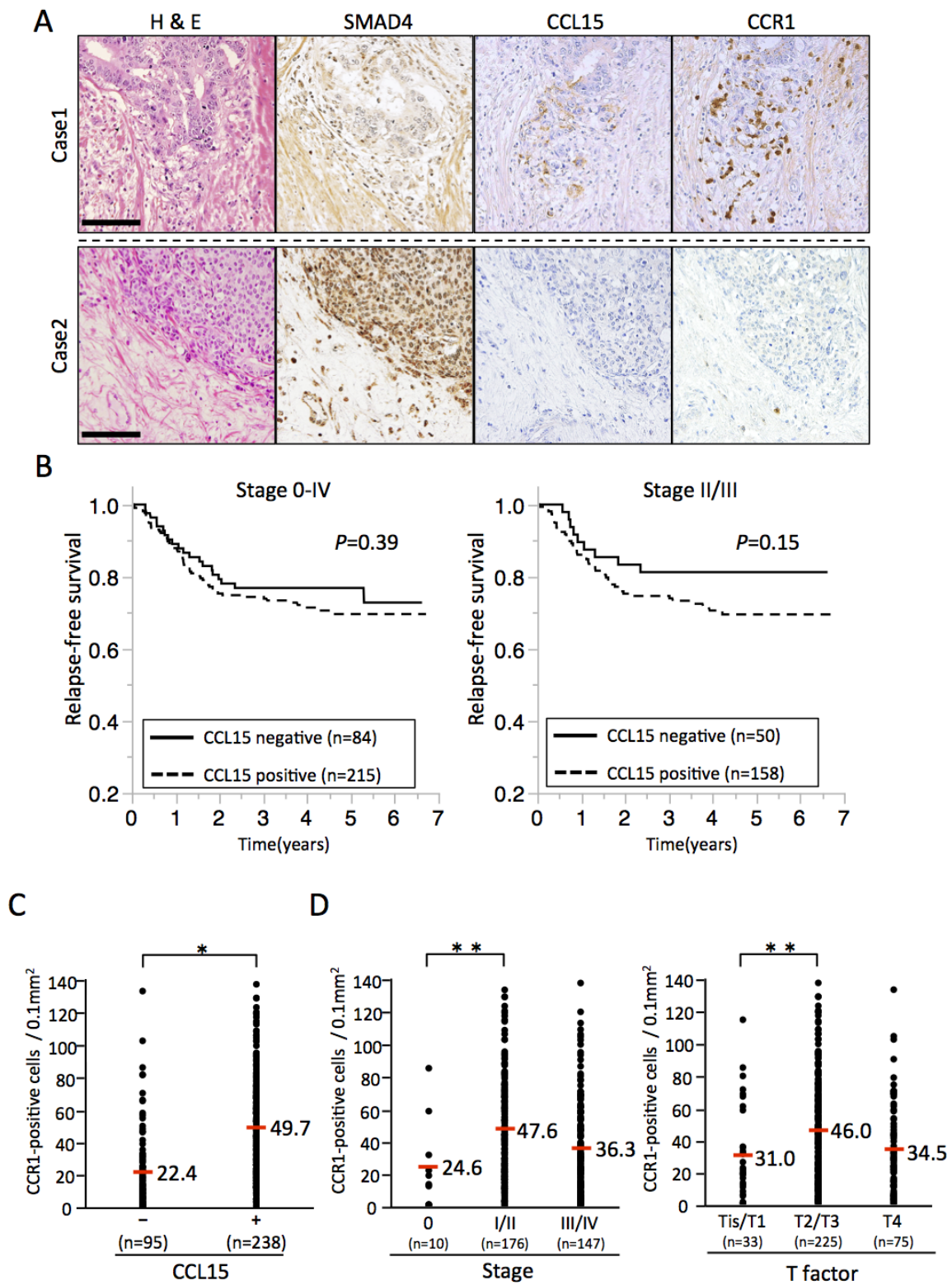
26

Figure 1

Figure 2

Figure 3
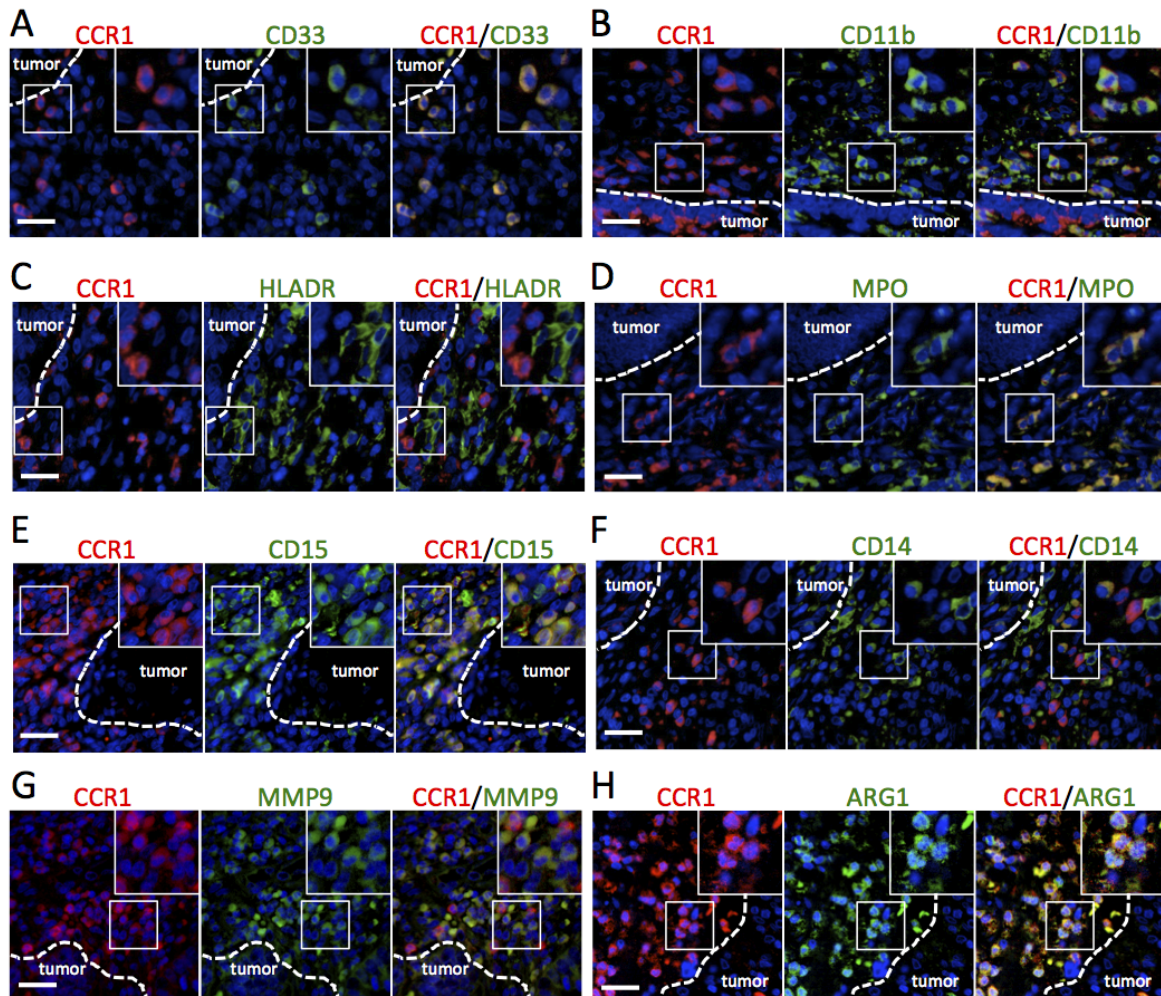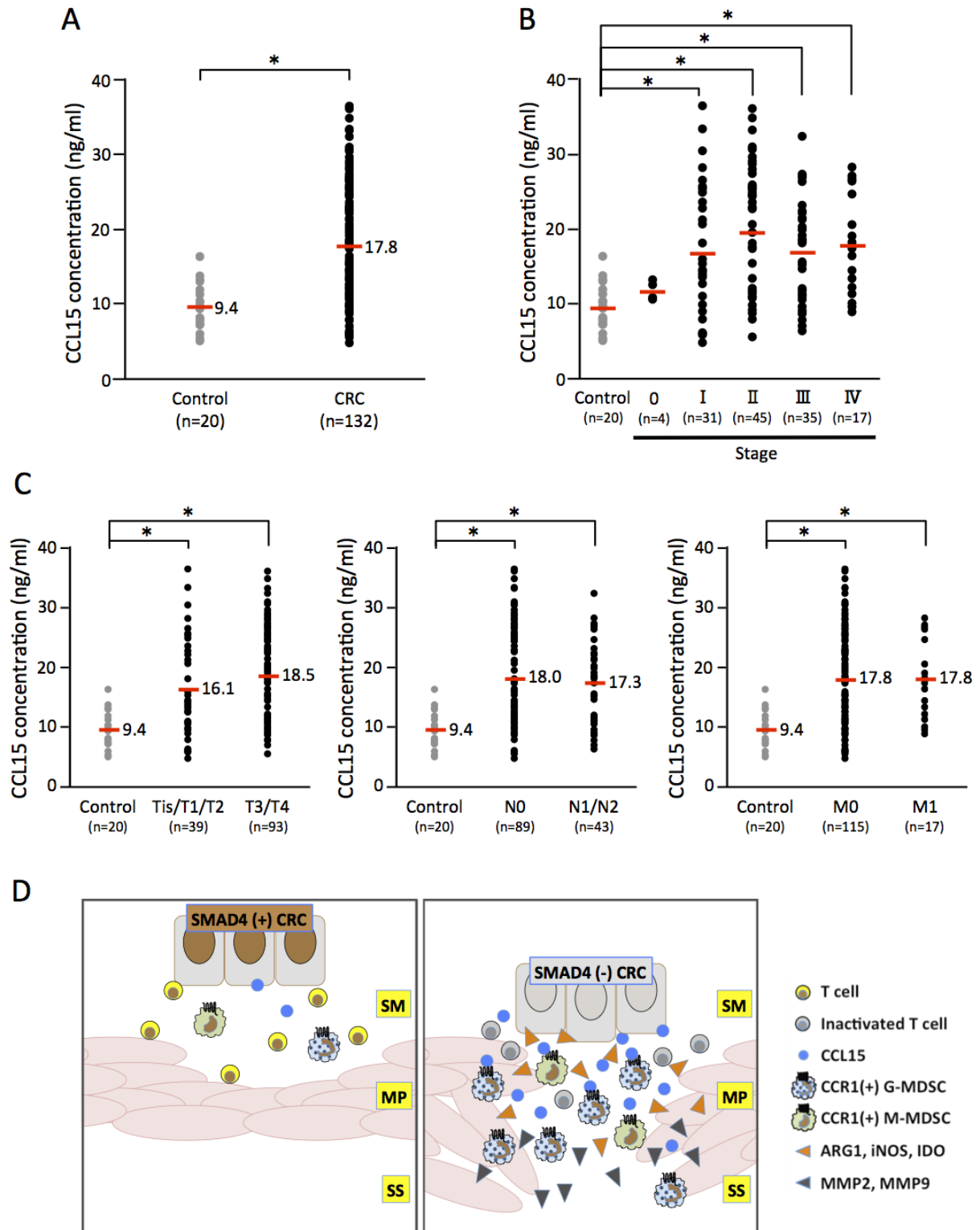
Figure 4

AACR American Association for Cancer Research

Clinical Cancer Research

Loss of SMAD4 Promotes Colorectal Cancer Progression by Accumulation of Myeloid-Derived Suppressor Cells through CCL15-CCR1 Chemokine Axis

Susumu Inamoto, Yoshiro Itatani, Takamasa Yamamoto, et al.

Updated version	Access the most recent version of this article at: doi:10.1158/1078-0432.CCR-15-0726
Author Manuscript	Author manuscripts have been peer reviewed and accepted for publication but have not yet been edited.

E-mail alerts	Sign up to receive free email-alerts related to this article or journal.
Reprints and Subscriptions	To order reprints of this article or to subscribe to the journal, contact the AACR Publications Department at pubs@aacr.org.
Permissions	To request permission to re-use all or part of this article, contact the AACR Publications Department at permissions@aacr.org.

Supplementary Table1. List of antibodies used for IHC, IF and western blotting.

Antibody	Host	Company	dilution ratio
anti-SMAD4	mouse	Santa Cruz	1:100
anti- CCL15	Guinea pig	made in our lab	1:100
anti-hCCR1	rabbit	Genway Biotech	1:100
anti-mCCR1	rabbit	made in our lab	1:500
anti-hMLH1	mouse	BD Pharmingen	1:50
anti-hMSH2	mouse	Calbiochem	1:100
anti-CD3	mouse	Lica	1:100
anti-CD8	mouse	Lica	1:100
anti-α-SMA	mouse	Sigma Aldrich	1:400
anti-CD68	mouse	Dako	1:100
anti-CD11b	goat	Santa Cruz	1:100
anti-CD14	mouse	Lica	1:50
anti-CD15	mouse	Lica	1:20
anti-MPO	mouse	Lica	1:100
anti-CD31	mouse	Dako	1:40
anti-CD33	mouse	Lica	1:100
anti-HLADR	mouse	Lica	1:50
anti-MMP2	mouse	Abcam	1:100
anti-MMP9	mouse	Santa Cruz	1:100
anti-CCR2	mouse	Abcam	1:500
anti-CCR3	goat	Abcam	1:200
anti-CXCR2	mouse	Abcam	1:100
anti-iNOS	mouse	R&D Systems	1:50
anti-ARG1	mouse	R&D Systems	1:50
anti-IDO	mouse	Abcam	1:100

Supplementary Table2. CCL15 expression of primary CRC according to the Stage- and T factor-based classifications.

Characteristics	CCL15 expression		Positive proportion (%)
	- (n = 95)	+ (n = 238)	
UICC-TNM Stage			
0	6	4	40.0
I	19	40	67.8
II	31	86	73.5
III	19	72	79.1
IV	20	36	64.3
T factor			
Tis	7	4	36.4
T1	9	13	59.1
T2	12	40	76.9
T3	42	131	75.7
T4	25	50	66.7

Supplementary Table3. Tumor characteristics. Preoperative serum samples from another cohort of 132 patients.

Characteristics	No. of Patients
Age, years	
Mean ± SD	66.6 ± 12.8
Sex	
Male	70
Female	62
Location	
Colon	89
Rectum	43
Histology	
tub1 / tub2	116
others	16
T factor	
Tis / T1 / T2	39
T3 / T4	93
N factor	
Negative	89
Positive	43
M factor	
Negative	115
Positive	17
UICC-TNM Stage	
0, I, II	80
III, IV	52
CEA, ng/mL	
< 5	85
≥ 5	47
CA19-9, U/mL	
< 37	111
≥ 37	21

Supplementary Figure legends

Supplementary Figure S1.

A, ELISA showing CCL15 concentration of conditioned medium when SMAD4 was overexpressed in Colo205 cells. Mean; bars, ± SD. (Student's *t*-test; *, $P < 0.05$). B, Quantification of the cell proliferation rates of HT29 (left) and Colo205 cells (right). Results are presented as mean ± SD of triplicate cultures.

Supplementary Figure S2.

A, Kaplan-Meier curves of overall survival (left) and RFS (right) in CRC patients. B, Effect of SMAD4 on RFS in CRC patients who underwent curative resection of Stage 0-IV (left) and Stage II/III CRC (right) (Kaplan-Meier estimates). C, Effect of MMR status on RFS in CRC patients who underwent curative resection of Stage 0-IV (left) and Stage II/III CRC (right) (Kaplan-Meier estimates).

Supplementary Figure S3.

Clinical specimens from 8 CRC patients (Stage I, n = 2; Stage II, n = 5; Stage III, n = 1) were analyzed. Immunofluorescence staining for CCR1 and A, CD3, B, CD8, C, α-SMA, D, CD31, E, CD68, F, MMP2, G, iNOS, H, IDO, I, CCR2, and J, CXCR2. Scale bar, 20 μm.

Supplementary Figure S4.

A, Haematoxylin and eosin staining (H&E) and IHC staining for SMAD4, CCL15, CCR1 and CCR3 of primary CRC specimens. Scale bar, 100 μm. B, Quantification of the CCR3$^+$ cell density in primary CRC with and without CCL15 expression ($n = 238$ and 95, respectively). Mann-Whitney U test; horizontal bands show the means. C, Quantification of the CCR3$^+$ cell density in primary CRC with and without SMAD4 expression ($n = 197$ and 136, respectively). Mann-Whitney U test; horizontal bands show the means. D, Scatter plot of CCR1$^+$ cell density and CCR3$^+$ cell density. The relationship between

variables was determined by Pearson's correlation coefficient (r = 0.031, P= 0.57).

Supplementary Materials and Methods

In vivo xenograft studies

  We injected 1.0×10^6 of cancer cells into the rectum of eight-week old female nude mice. For *in vivo* bioluminescence imaging, we injected 3 mg of D-luciferin (VivoGlo luciferin, Promega, Madison, WI) intraperitoneally into anesthetized tumor-bearing mice 10 min before imaging. Bioluminescence from the luciferase-expressing tumor cells was scored at days 7, 14, 21, 28 and 35 post-injection, using a Xenogen IVIS system (Xenogen Corporation, Alameda, CA). All animal experiments were approved by the Animal Care and Use Committee of Kyoto University.

Lentiviral transduction

  The specific oligonucleotides were used to knockdown *CCL15*, as previously described (7, 9). Each set of oligonucleotides were annealed and cloned into the *AgeI/EcoRI* sites of pLKO.1 (Addgene, Cambridge, MA). For the control knockdown sequence, we employed pLKO.1-scrabmle plasmid (Addgene #1864). Firefly luciferase and cMyc-tagged human *SMAD4* were cloned into lentivirus plasmid pLEX-MCS (Addgene) as previously described (9). These plasmids were transfected with virus particle vectors (psPAX2 and pMD2.G (Addgene)) to produce recombinant lentiviruses. After cloning of stable transductants of HT29 cells for firefly luciferase (Luc-HT29 cells), recombinant lentiviruses were introduced into them, followed by hygromycin selection (500 μg/ml) as a pool to minimize clonal variation.

Cell viability assay

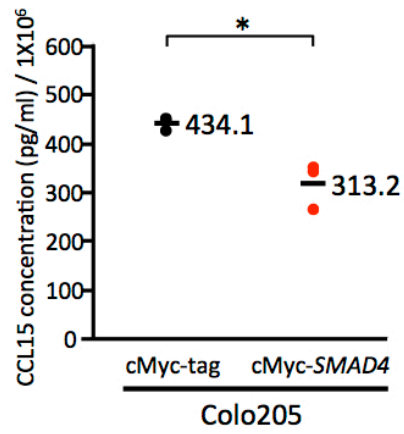 Tumor cells (1.0×10^5 cells) were incubated in triplicate for 24, 72 and 120 h in 10% fetal bovine serum. Viable cells were counted by the trypan blue dye exclusion method. Three sets of experiments were performed for each set.
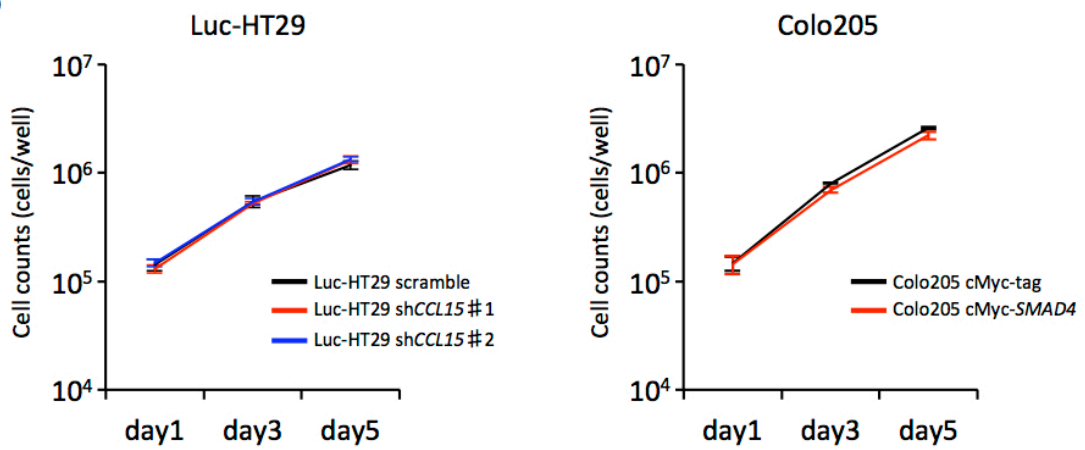
Enzyme-linked immunosorbent assay (ELISA)

Preoperative serums were diluted 50 times, and then serum CCL15 levels were measured using ELISA Human CCL15 DuoSet (R&D Systems, Miinneapolis, MN) according to the manufacturer's protocol. CRC cell lines were incubated for 72 h, and then secreted CCL15 into conditioned medium was measured by the same method. In some cases, we examined serum CCL15 levels in both fresh and frozen samples from the same patients, and found similar levels of CCL15 expression.
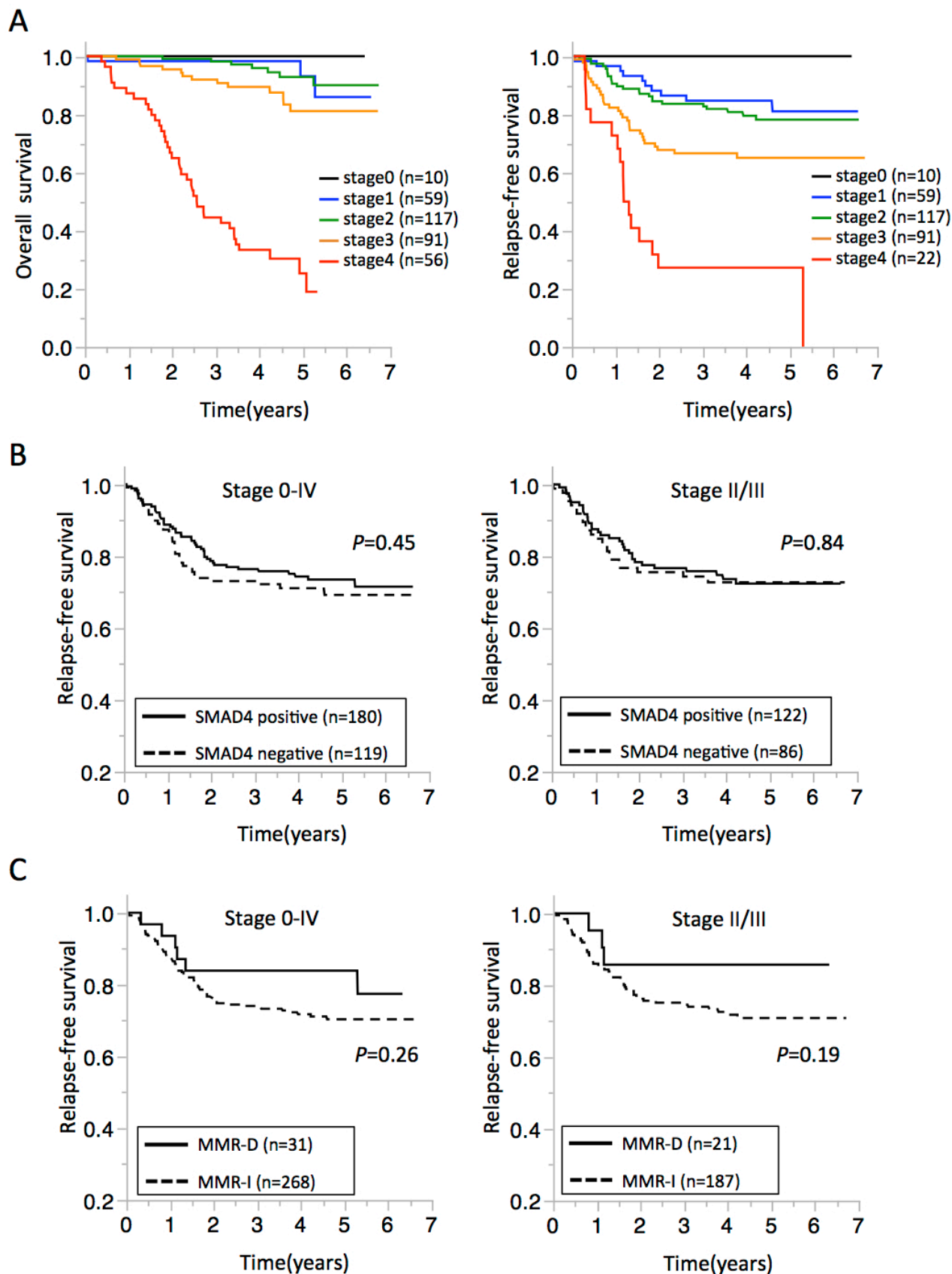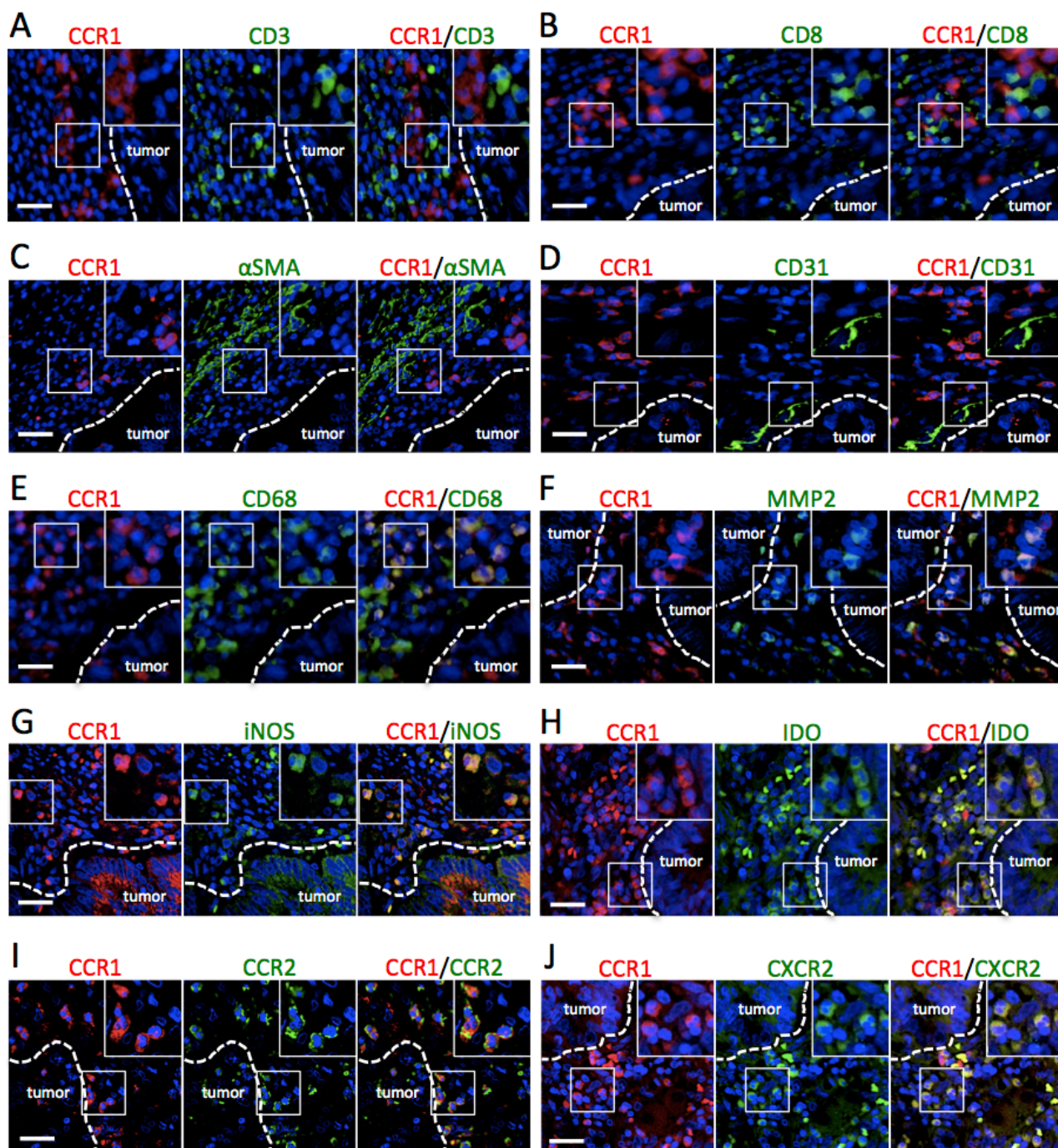
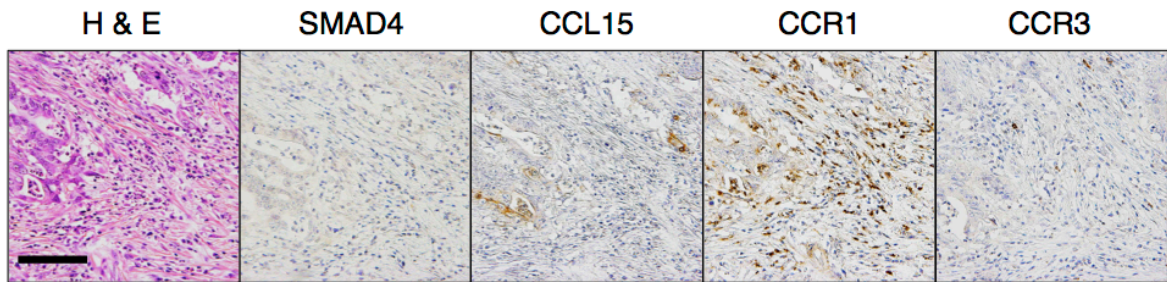# Supplementary Figure S1

A

B
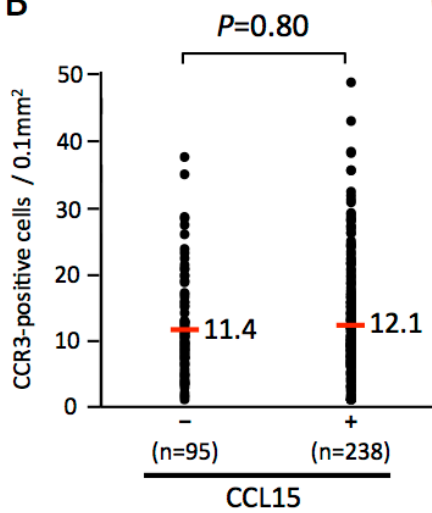
Supplementary Figure S2

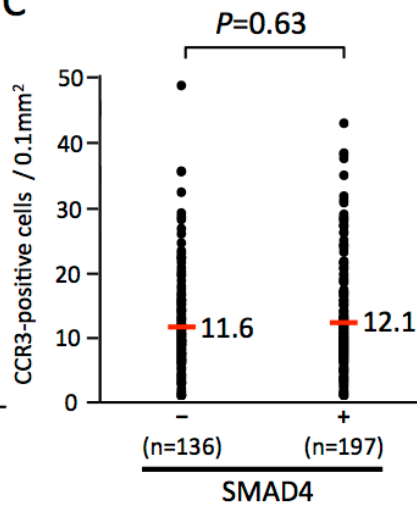# Supplementary Figure S3

Supplementary Figure S4

A

| H & E | SMAD4 | CCL15 | CCR1 | CCR3 |

B

P=0.80

CCR3-positive cells / 0.1mm²

— 11.4

— 12.1

−
(n=95)

+
(n=238)

CCL15

C

P=0.63

CCR3-positive cells / 0.1mm²

— 11.6

— 12.1

−
(n=136)

+
(n=197)

SMAD4

D

P=0.57
r=0.031

CCR3-positive cells / 0.1mm²

CCR1-positive cells / 0.1mm²